

## CROSS-CORRELATION OF VELOCITY MEASUREMENTS FOR WIND RESOURCE ASSESSMENT OVER A LARGE COMPLEX TERRAIN

Constantine J. Stratiridakis\*  
S.A.M.-High Technology Consulting and Applications S.A.  
1770 str. No. 12, Heraklion GR-71202, GREECE

Bruce R. White<sup>†</sup> and Jorge Gonzalez<sup>‡</sup>  
Department of Mechanical and Aeronautical Engineering  
University of California  
Davis CA. 95616, USA

### Abstract

In the present experimental investigation, the wind resource over a 5 km<sup>2</sup> complex-terrain potential site of a Wind Farm is being measured. For the wind measurements a new methodology is being introduced, in order to minimize the number of weather stations necessary to monitor the wind conditions and to increase the validity of the weather station measurements over a much wider range. The methodology is based on two-point space-time correlation measurements of the instantaneous velocity field. Hot-wire anemometry was utilized in the Atmospheric Boundary Layer Wind Tunnel at UC Davis for the measurements. On site, correlation measurements were performed using two weather stations, one station was fixed and the other was portable. Since the correlation measurements do not require long measurement periods, the method appears to be inexpensive and gives reasonable velocity-field assessments over large complex sites using minimum number of measurement stations. The spatial correlation results gave more insight in the wind-flow field characteristics and pointed out locations, where a network of weather stations could be installed, for improving the tools for the creation of more reliable future prediction models for the wind resource assessment.

### Introduction

Accurate wind forecasting could save utilities tens of millions of dollars a year by predicting wind generation of the next day<sup>1</sup>. Over a complex terrain of several km<sup>2</sup>, wind

resource assessment is an expensive and time-consuming process<sup>2,3</sup>.

Large and rapid changes in wind speed cause corresponding changes in wind power production, thus serious reduction in utility operating economy and reliability occurs, especially for utilities with large wind-power penetration like on the island of Crete (approximately 30%). Utilities could use reliable prediction of wind power to schedule the connection or disconnection of wind or conventional generation, achieving low-spinning reserve at optimum operating cost<sup>4</sup>.

Spatial correlation studies conclude that significant correlation of hourly or daily-mean wind speed exists, for distances up to 100 kilometers<sup>5</sup>. The spatial correlation decreases with distance, and when the orientation of the distance vector differs from the wind direction<sup>6</sup>. The correlation coefficients are related to the wind direction, terrain roughness and height above the ground<sup>7</sup>.

In the present investigation, spatial correlation measurements were utilized for determining the velocity correlation, which exists over a large complex terrain. Spatial correlation could lead to wind-speed prediction at locations, where no long-term wind-speed measurements exist, by correlating these measurements with measurements at a reference location, where long-term wind-speed data exists. This method could be proven to be valuable for wind resource assessment and in predicting the wind-power output of wind turbines sited on a complex terrain.

---

\* Managing Director, Senior Member AIAA

<sup>†</sup> Professor, Fellow Member AIAA.

<sup>‡</sup> Graduate student; on exchange program from University of Madrid Spain.

Copyright © 1999 by the American Institute of Aeronautics and Astronautics Inc. And the American Society of Mechanical Engineers All rights reserved.

For the correlation measurements conducted in this study, the U.C. Davis Atmospheric Boundary Layer wind tunnel was used (*Figure-1*). The wind tunnel measurements were

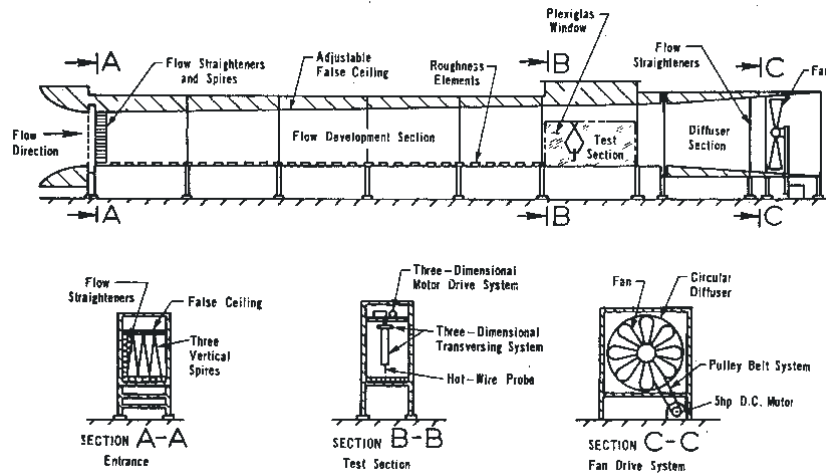


*Figure - 1. The UC Davis Atmospheric Boundary Layer Wind Tunnel.*



*Figure - 2. The scaled (1:5,000) model of the site placed in the wind-tunnel.*

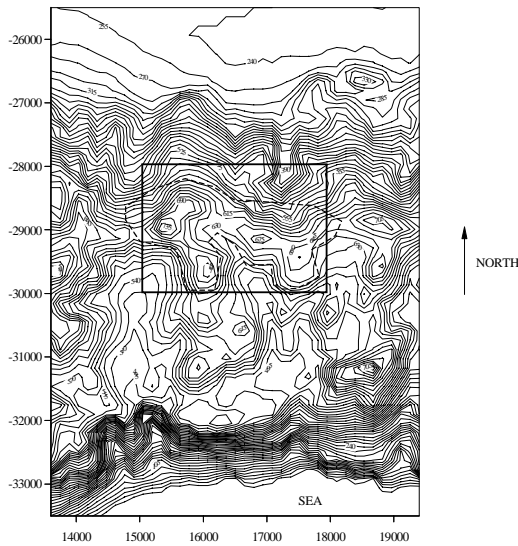


Figure - 3. Top view of the site in cartesian coordinates (m).

validated at one location with full-scale field data. The UCD wind tunnel is suitable in simulating full-scale winds<sup>2,3,8</sup>. A 1:5,000 model of the terrain under investigation was placed in the wind tunnel (Figure-2 and Figure-3) and velocity, turbulence and correlation measurements were conducted. It is important to note that the UCD wind tunnel is simulating the air flow in the lowest few hundred meters of the atmosphere.

The complex-terrain site is on the southern coast of Crete, the largest Greek island, where a 20 MW Wind-Farm project is under development. For this project, a 5 km<sup>2</sup> mountainous land is available. The permanent weather station on the site has shown that the yearly average wind is approximately 9.0 m/s at 10 m above ground level. The prevailing winds are mostly North and to a lesser extent South. North of the site, extends a large valley (10 km across), while after 4 km to the south, one meets the high cliffs (500 m elevation) of the southern coast of the island<sup>2</sup>.

Hot-wire anemometry was used to perform velocity, turbulence and spatial correlation measurements at 8 locations over the model. A single hot-wire probe was positioned at the fixed location of the permanent weather station (fixed probe) and the second probe (portable probe) was positioned at various locations over the site for the spatial correlation measurements. At every location, measurements were made at two different heights, corresponding to 10 and 40 full-scale meters, respectively.

Currently, the wind-tunnel data are been verified by field measurements using the permanent weather-station data

and measurements from a second, portable weather station at 10m height.

## Experimental Facility and Techniques

### The UC Davis Atmospheric Boundary Layer Wind Tunnel

In this study, the UC Davis Atmospheric Boundary Layer Wind Tunnel (ABLWT) was used (Figure-1). The wind tunnel is able to simulate naturally turbulent boundary layers, such as wind flow near the surface of the earth and it is composed of four sections: the entrance, the flow developing section, the test section, and the diffuser section.

The entrance section is of elliptical shape and provides this way the incoming flow with a smooth contraction area, which minimizes the turbulence. A commercially available air filter follows the contraction area. This filter reduces large-scale pressure fluctuations of the flow and filters larger-size particle out of the incoming flow. After the filter, a honeycomb flow straightener is used to reduce large-scale turbulence.

The second part of the wind tunnel is the flow development section. It is 12.2 m long and produces mature turbulent boundary layer. Four spires mounted at the entrance of this section and surface roughness elements placed all over the surface of this section generate a boundary layer height of one meter at the test section. The ceilings of the developing and test sections are adjustable and together with the diverging walls of the developing section, provide zero-pressure-gradient flow.

The dimensions of the test section are 3 m in streamwise length, 1.7 m high and 1.2 m wide. The test section can be observed from both sides through a framed Plexiglas window and a framed Plexiglas door, which allows access to the test section. To introduce a probe in the test-section a three-dimensional traversing system is installed at the ceiling of the test section. The sensor can be moved over almost the whole test section volume. The traversing system is of aerodynamically shape minimizing influences on the flow. The centerline wind speeds within the test section can be adjusted from 1 m/s to 10 m/s.

The diffuser section is 2.44 m long. It has a circular cross section for the fan. The eight-blade, fixed-pitch, 1.83 m-diameter fan is powered by a 56 kW DC motor with controller.

### The wind-tunnel characteristics

The boundary layer in the wind tunnel is turbulent like the atmospheric boundary layer and this has been achieved by the roughening elements on the long developing section,

so that the roughness Reynolds number,  $Re_z$  ( $Re_z = u_* z_0 / \nu$ ) is greater than 2.5. The UC Davis ABLWT satisfies this condition, since the roughness Reynolds number is about 40; when the wind-tunnel freestream velocity,  $U_\infty$ , is equal to 3.8 m/s, the friction speed,  $u_*$ , is 0.24 m/s and the roughness height,  $z_0$ , is 0.0025 m. Thus, with the freestream speed of 3.8 m/s the flow satisfies the Re number independence criterion and dynamically simulates the flow. The other criteria (Jensen's length scale criterion and the model to be constrained within 15% of the wind-tunnel boundary layer height) are met<sup>2</sup>.

Figures-4 through -6 present the wind-tunnel mean velocity, turbulence intensity and spectra characteristics, respectively, at the entrance of the test section, as compared with full-scale data.

### Experiment Description

In the present investigation, it is aimed to determine the spatial correlation between a reference point, where long-term meteorological measurements are known, and other locations within the 5 km<sup>2</sup> site, where no long-term observations exist. The reference point was chosen to be the location of the permanent weather station. This reference location is marked as No. 23 (ref. to Figure-7).

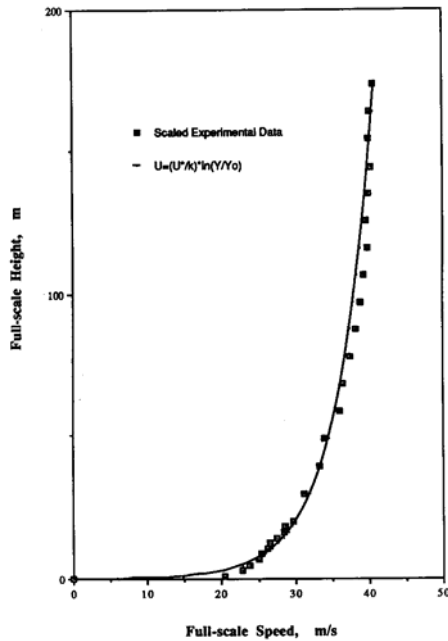


Figure-4: Mean Velocity (m/s)

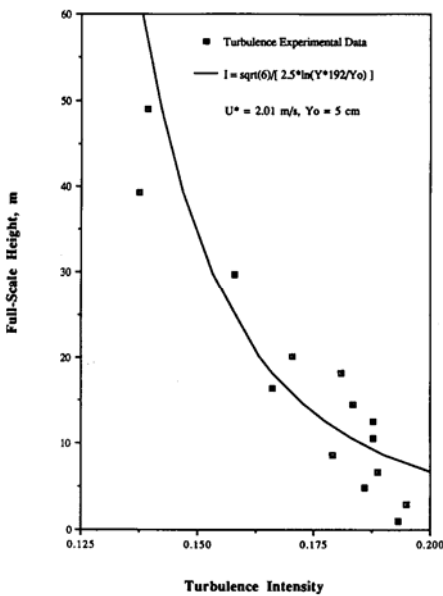


Figure-5: Turbulence Intensity

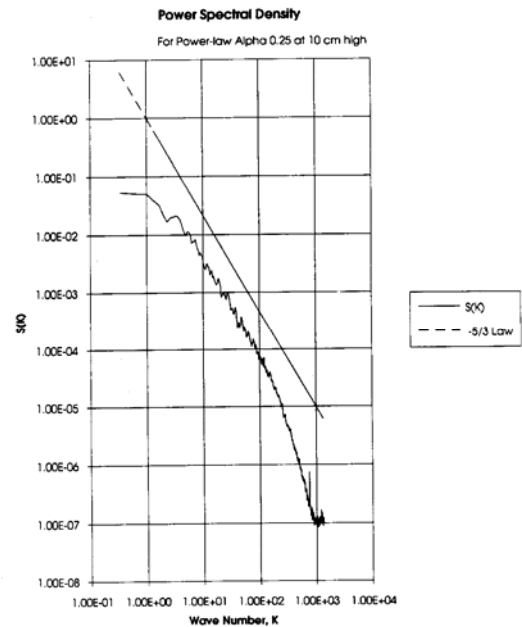
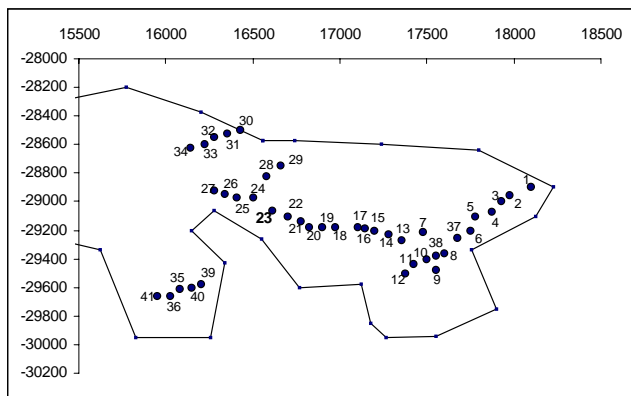


Figure-6: Power Spectral Density

The same point corresponds to the position of the fixed hot-wire probe for the wind-tunnel testing.

Strataridakis et al.<sup>2</sup> in a previous investigation determined the high wind-energy areas in the flow field over the predetermined site. Since the prevailing winds over the site are North and South (over 85% of occurrence), the high energy contours for these two wind directions were superimposed and the common high-energetic area was determined. The wind-tunnel testing was performed within this area of the flow field. Figure-7 identifies the testing locations. The same Figure outlines the site boundary, which coincides with the boundary shown on the map of Figure-3.

Mean velocity and turbulence measurements were taken at forty-one locations over the model site, which was placed in the wind tunnel and tested for the two prevailing-wind directions. The experiment was repeated for three heights, i.e., at 10, 20 and 40 m above ground level.



**Figure-7:** Wind-Tunnel Testing Locations within the Site. The coordinates are Cartesian (m)

In the wind tunnel, spatial correlation measurements were performed using two single hot-wire probes. One probe was fixed at the reference location No.23 and the other portable probe was positioned at locations No. 35, 32, 26, 28, 19, 15, 10 and 4, respectively. The fixed and portable probes were simultaneously positioned at 10 m and 40 m a.g.l., respectively. Additional testing was performed keeping the fixed probe at 10 m and the portable one at 40 m a.g.l. and the fixed probe at 40 m and the portable probe at 10 m a.g.l.

Hot wire anemometry was used for the wind-tunnel testing: Two standard TSI single-sensors (TSI Model 1210-60); a two-channel thermal-anemometry unit with signal conditioner (TSI model IFA 100); and a 12 bit A/D converter (IBM Data Acquisition and Control Adapter DACA), driven by an IBM-AT computer. The hot-wire sensor was calibrated with the TSI-1125 calibration unit. The number of velocity samples and the sampling rate were equal for all wind-tunnel test runs. 90,000 samples were

acquired per point and they were taken with a rate of 1000 Hz, in order to satisfy the Nyquist sampling theorem, since the tunnel turbulence signal was 300 Hz. Thus the sampling time was 90 sec per point. Figure-8 presents the schematic diagram of the system used:

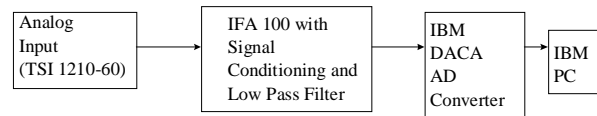


**Figure-8:** Schematic Diagram of the Wind-Tunnel Measurement System.

The on-site measurements were carried out using a fixed and a portable weather station. Anemometers were mounted at 10 m above ground level on both stations. The weather stations were monitored by two *S.A.M.-MTDL552-84* microcontroller-based 8-bit dataloggers. The dataloggers were real-time synchronized and communicated via a GSM modem at 9600 baud rate. The fixed weather station was located at point 23, while the second, portable weather station was positioned in location 35 and 19, sequentially.

### Uncertainties

Detailed uncertainty analysis is beyond the scope of this study, however, uncertainties in the wind-tunnel measurements were estimated to be:

Quantity	Uncertainty
Mean velocity	± 1%
Turbulence Intensity	± 5%
Spatial Correlation	± 7.5%
Probe positioning (horizontally)	± 7.5%
Probe positioning (vertically)	± 15%

**Table-1.** Uncertainty estimates.

### Exploring and Classifying the Mean Velocity, Turbulence and Wind-Shear Data

Exploratory and Cluster analysis has been applied to select the best locations for wind energy applications on the site. Mean velocity and turbulence data was collected at the Atmospheric Boundary Layer wind tunnel at three different heights for the two primary wind directions at 41 locations. Several statistical techniques mined and grouped these locations according to their wind power potential.

The objective of this analysis was to classify and select the best locations by applying different statistical techniques to explore, reduce and group the data taken. Three different statistical techniques were used to explore

and reduce the 12 variables considered in the analysis, that is, the wind speed and turbulence taken at 10, 20 and 40 full-scale meters for the North and South wind directions. These techniques were *Principal Components (P.C.)*, *Canonical Correlation* and *Factor Analysis*.<sup>9,10,11</sup>

The presentation of the detailed statistical analysis is beyond the scope of this paper, however, the major results of the analysis are summarized, herein.

The analysis of the correlation matrix shows that the speed variables are strongly correlated, especially the ones with the same wind direction. The correlation among the turbulence ones is much smaller. The cross-correlation of both is mostly negative, but very small.

The information gained with these techniques can be outlined as:

- Speed variables present similar characteristics and can be grouped together.
- The turbulence variables may also be grouped together but their similarities are weaker.
- A North-South variable division might be acknowledged.
- Among the turbulence variables, the 10 full-scale meter South-wind turbulence seems to be the most significant.
- Variables closer to the ground have more variability.

With this knowledge, one reasonable partition of the data would be splitting and averaging them into speed / turbulence and North / South variables. These 4 new averages could be further combined by noting that the frequency of the North wind is two times bigger than the South in the site of interest. Weighting the North speed and turbulence averages double than the South ones reduces the variables to a weighted-averaged-speed variable and a weighted-averaged-turbulence one.

It is known that for wind energy applications, the most important magnitudes are the speed and turbulence at the hub height (usually 40 meters). Another important variable is the wind shear, estimated by taking the difference in wind speed between the hub and the tip of the blade (around 20 meters). It is also common practice to consider the Turbulence Intensity (T.I.), that is, the proportion between the turbulence and the speed, to refer to the turbulent characteristics of the flow.

In order to present the data obtained in the Wind Tunnel independently of the particular testing conditions, three variables have been selected:

- 1- A speed-related variable, obtained by dividing the speeds at 40 full-scale meters by the maximum speed at each wind direction (North and South). These values have been averaged considering the wind frequencies in the site of study.

- 2- A turbulence-related variable, that is the Turbulence Intensity at 40 full-scale meters weighted by the frequency of the wind direction.
- 3- A shear-related variable, computed as the difference between the speed at 40 and 20 full-scale meters, divided by the speed at 40 m. The wind directions are weighted proportionally to their relative frequencies.

Hereafter, these three variables are mentioned as Combination Data. Among the three, the speed-related variable has the major role in selecting the best locations for the wind turbines.

### Cluster Analysis

Three clustering techniques have been applied with the Combination Data in order to classify and select the best locations: the *Hierarchical Agglomerative Single Linkage* and *Ward's sum of square error*, and the *Partitioning K-means method*.<sup>9,10,11</sup>

The output of the Single Linkage method is not satisfactory because of its poor cluster-definition due to the 'chaining' effect. The Ward's method splits the data into three main clusters, which classify the data in a meaningful way. The K-means technique was applied looking for N=2,3,4,5 clusters. The optimum number of clusters is 3. It divides the data consistently with the Ward's method but broadening one of the clusters. *Figure-9* summarizes the results of this statistical analysis.

The same analysis was repeated over the original 12 variables and the results are equivalent. Again, the single linkage approach was poor. The Ward's and K-means classifications agreed; in this case, the optimum was 4 clusters.

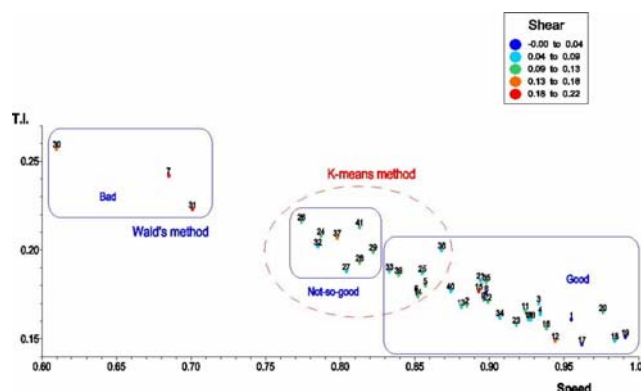


**Figure-9:** Combination data classified with Ward's and K-means methods

### Data Classification for the Best Locations for Wind-Turbine Sites

With the above considerations and maintaining the original data as the final reference, the 41 locations have been classified in:

- Good: 5, 6, 39, 14, 25, 36, 33, 21, 22, 2, 35, 13, 40, 9, 34, 8, 4, 10, 3, 38, 23, 1, 17, 19, 18, 20, 11, 16, 12, 15.
- Not-so-good: 27, 32, 28, 41, 29, 24, 26, 37.
- Bad: 7, 31, 30.

It is observed that the results of this statistical analysis coincide with the results of Stratiridakis et al.<sup>2</sup> using turbulence measurements and wind power calculations.

### Spatial Correlation Measurements

In the present experimental investigation, the wind resource over a 5 km<sup>2</sup> potential site of a Wind Farm was measured. For the wind measurements a new methodology was introduced, in order to minimize the number of weather stations necessary to monitor and hence, predict the wind conditions and to increase the validity of the weather station measurements over a much wider range of a complex terrain. The methodology was based on two-point space-time correlation measurements of the instantaneous velocity field.<sup>12,13</sup> Hot-wire anemometry was utilized in the U.C. Davis Atmospheric Boundary Layer Wind Tunnel for the measurements. On site, correlation measurements were performed using two weather stations, one station was fixed and the other was portable. Since the correlation measurements do not require long measurement periods, the method appears to be inexpensive and gives reasonable velocity-field assessments over large complex sites using minimum number of measurement stations.

The cross-correlation function  $R_{q,q}$  serves as a quantitative measure of the similarity between the two time series. The  $R_{q,q}$  function may be defined in the equation below as:

$$R_{q,q} = \frac{\langle q(x,y,z,t) q(x+\Delta x, y+\Delta y, z+\Delta z, t+\Delta t) \rangle}{q_{rms}(x,y,z,t) q_{rms}(x+\Delta x, y+\Delta y, z+\Delta z, t+\Delta t)} \quad (1)$$

where  $q$  can be either  $u'$ , or  $v'$ , or  $u'v'$ ;  $q_{rms}$  is the RMS value of  $q$ ;  $(x,y,z)$  is the location of one probe in space and the second probe is separated by the first one by  $(\Delta x, \Delta y, \Delta z)$ . The time coordinate is  $t$  and  $\Delta t$  is the variable time shift and the  $\langle \rangle$  indicate time averaged quantities.

In the following Figures, the spatial correlation data are presented. The fixed probe ( $f$ ) was at location 23 (ref. Figure-7), while the portable probe ( $p$ ) was positioned over locations 4, 10, 15, 19, 28, 26, 32 and 35, respectively, at heights of 10 and 40 m a.g.l.

Every spatial correlation figure shows two plots, the heavy-line plot represents the data with the portable probe

positioned at 10 m a.g.l., while the lighter-line plot represents the data with the portable probe at 40 m a.g.l. The corresponding height of the fixed probe along with the wind direction is written on the top of each figure. The horizontal axis  $Dt$  is the time shift in the two hot-wire probe signals, indicated by sampling-time shifts. The real time shift is given by:

$$Dt_{real\ time} = Dt/f \quad [sec] \quad (2)$$

where  $Dt$  plotted on the figures is the number of samples shifted and  $f$  is the sampling frequency [Hz] (i.e.,  $f=1,000$  Hz).

Whenever, a distinct peak appears on a spatial correlation figure, the  $Dt_{peak}$  gives an estimate of a coherent wind-flow structure propagating at a mean speed  $u(t)$ , which equals to:

$$u(t) = d/Dt_{peak} \quad [m/sec] \quad (3)$$

where  $d$  is the distance between the fixed and the portable probes along the wind direction in [m] and  $Dt_{peak}$  is in [sec].

Figures 10 and 11 show the spatial correlation at location 35 for North and South wind respectively. For both wind directions the data indicate that the flow appears more coherent at 10 m, since local flow effects are stronger, while the wind flow at hub heights (40 m) is more independent. This result suggests that another anemometer at 40 m high should be placed on the hill about location 35.

Figure-12 presents the flow independence for North winds over point 32, while Figure-13 shows that for South winds, over the same location, the flow has similarities that are invariant with respect to the height.

Figures 14 through 17 present the correlation at point 26. All graphs indicate that there is some consistent dependency of the flow over points 23 and 26. The correlation is independent of height. Both points are on the top of hills, but with different surrounding topography. The correlation is negative for North winds and positive for South winds and this is due to the local flow effects. Therefore, the measurements at location 23 could be used for estimating the wind speeds over location 26.

Figures 18 and 19 show that there is a distinct flow coherence for North winds and this is due to the fact that point 28 is in the vicinity upstream point 23. The correlation almost doubles when both probes are at 40 m full scale. This is expected because local flow effects become less important. Figure-20 shows that there is no correlation for the flow over points 23 and 28 for South winds. This is expected because point 28 is within the recirculation region of the hill that point 23 is on. At the height of 40 m, there is strong correlation, almost identical, for South winds. This means that there is very little distortion of the flow at those heights. The small twin peak that can be distinguished in the correlation when both probes are at 40 m, indicates that there is some specific

flow- direction fluctuation due to the upstream topography. In this case, data from the weather station at 23 could be used for estimating wind speeds at point 28 (hub heights).

Figures 22 through 24 show the correlation over points 23 and 19. There is flow coherence over these points. For North winds, the flow appears to be a little dependent on the height, however, for South winds the flow is almost independent of height. Because point 19 is at the top of a hill and the surroundings are at lower heights, apparently there is a flow-direction fluctuation, as the twin-peak spatial correlation at that point indicates.

Figures 25 and 26 present that, for North winds, there is small flow coherence at low heights only. At this point a weather station should be placed, also.

Figures 27 and 28 indicate that points 10 and 4 are not coherent in respect to the wind flow, thus more weather stations should be placed there to accurately measure the full-scale flow field.

In this study all other spatial correlation that was measured and not presented here was insignificant, that is the reason not included in this paper. The full-scale space-time correlation measured over points 23 and 35 was low as Figure-10 indicates.

### Summary

Reliable prediction of wind resource is vital information to utilities to schedule the connection or disconnection of wind or conventional power generation, at optimum operational cost. This is important especially for utilities with large wind-power penetration, like on the island of Crete (30%). In order to apply, safely, wind-resource prediction models, the wind-flow field over large complex terrain areas must be accurately measured using a network of weather stations. Over a complex terrain, it is economical and practical to utilize spatial correlation measurements of the wind-speeds at different locations and heights, in order to determine at which strategic locations it is necessary to install weather stations for the wind-resource assessment.

In the present investigation, hot wire anemometry was used to acquire wind-speed, turbulence, wind shear and spatial correlation measurements over a scaled model (1:5,000) of a large complex-terrain site. The model of a potential Wind-Farm site was placed in the test section of the U.C. Davis Atmospheric Boundary Layer Wind Tunnel for physically simulating the flow.

Cluster analysis was performed to classify the mean velocity, turbulence and shear data. The statistical result, coincided with previous results of Strataridakis et al.<sup>2</sup> regarding the specific site.

The spatial correlation results gave more insight in the wind-flow field characteristics and pointed out the locations that are independent of the direct measurements at a reference location, i.e., the permanent weather station on

the site. Thus, locations were identified, where a network of weather stations could be installed, in order to improve the tools for the creation of more reliable future prediction models for the wind resource assessment.

### References

1. The Federal Wind Energy Program, *Wind Power Today*, US Department of Energy, pp. 32-33, 1997.
2. Strataridakis, C.J., White B.R., and Greis A., *Turbulence Measurements for Wind-Turbine Siting on a Complex Terrain*, Proceedings of the Joint AIAA/ASME Wind Energy Conference, Paper WE-99-0054, Reno, NV, 1999.
3. Migliore, P.G., Obermeier, J., White, B.R., *Wind Tunnel Testing as an Aid in Site Assessment*, Winpower '85, San Francisco, 1985.
4. Damousis, I.G., Dokopoulos, P.D., *A Generic Fuzzy Model for Wind Speed Prediction and Power Generation in Wind Parks, Secure Wind Power Penetration in Isolated Systems*, CARE Workshop, European Commission Direction General XVII, JOULE Project, Heraklion Crete 16-17 July 1999.
5. Corotis, R., Sigl, A., Cohen M. *Variance Analysis of Wind Characteristics for Energy Conversion*, Journal of Applied Meteorology, v. 16, pp.1149-1157, 1977.
6. Palomino, I., Martin, F., *A Simple Method for Spatial Interpolation of the Wind in Complex Terrain*, Journal of Applied Meteorology, v.34, pp. 1678-1693, 1995.
7. Chan, S.M., Powell, D.C., Yoshimura, M., Curtice, D.H., *Operations Requirements of Utilities with Wind Power Generation*, IEEE Transactions on Power Apparatus and Systems, v.102, No. 9, 1983.
8. White, B.R., *Physical modeling of atmospheric flow and environmental applications*, Proceeding of the 51<sup>st</sup> Anniversary Conference of KSME, 1996.
9. Dillon, W.R. and Goldstein, M., *Multivariate analysis. Methods and applications*. Wiley, 1984.
10. Johnson, R.A. and Wichern, D.W., *Applied multivariate statistical analysis*, Prentice-Hall, 1998.
11. Everitt, B.S. and Dunn, G. (1991) *Applied multivariate data analysis*. Edward Arnold, 1991.
12. Strataridakis, C.J., White B.R., Robinson S.K., *Experimental Measurements of Large Scale Structures in an Incompressible Turbulent Boundary Layer Using Correlated X-Probes*, AIAA-89-0133, Reno, NV, 1989.
13. Hinze, J.O., *Turbulence*, McGraw-Hill, 1987.